This document is the Accepted Manuscript version of a Published Work that appeared in final form in **Applied Physics Letters** 104(23) : (2014) // Article ID 231905, copyright © 2014 AIP Publishing after peer review and technical editing by the publisher. To access the final edited and published work see https://doi.org/10.1063/1.4882903

Vacancy dynamic in Ni-Mn-Ga ferromagnetic shape memory alloys

D. Mérida[1,2], J. A. Garcia[1,4], V. Sanchez-Alarcos[3], I. Pérez-Landazábal[3], V.Recarte[3] and F. Plazaola[2]

[1]Fisika Aplikatua II Saila, Euskal Herriko Unibertsitatea UPV/EHU, p.k. 644, 48080 Bilbao, Spain

[2]Elektrizitate eta Elektronika Saila, Euskal Herriko Unibertsitatea UPV/EHU, p.k. 644, 48080 Bilbao, Spain

[3]Departamento de Física, Universidad Pública de Navarra, Campus de Arrosadia, 31006 Pamplona, Spain

[4]BC Materials (Basque Centre for Materials, Application and Nanostructures), 48040 Leioa, Spain

*Corresponding Author: D. Mérida

E-mail Address: david.merida@ehu.es

Abstract

Vacancies control any atomic ordering process and consequently most of the order-dependent properties of the martensitic transformation in ferromagnetic shape memory alloys. Positron annihilation spectroscopy demonstrates to be a powerful technique to study vacancies in NiMnGa alloys quenched from different temperatures and subjected to post-quench isothermal annealing treatments. Considering an effective vacancy type the temperature dependence of the vacancy concentration has been evaluated. Samples quenched from 1173 K show a vacancy concentration of 1100±200ppm. The vacancy migration and formation energies have been estimated to be 0.55±0.05eV and 0.90±0.07eV, respectively.

Keywords: *Ni-Mn-Ga alloys, Vacancies dynamics, Ferromagnetic Shape Memory Alloys, Martensitic transformation*

Since giant magnetic-field-induced strain (MFIS) was first reported on Ni-Mn-Ga ferromagnetic shape memory alloys (FSMA) by Ullakko et al. [1] a great amount of work has been performed to understand and improve functional properties of this alloy system in order to be implemented in practical devices [2-3]. Their particular properties are linked to the presence of a thermoelastic martensitic transformation (MT). The MT temperature strongly depends on composition and the compositional dependence has been described as a function of the electron to atom ratio, e/a [4]. Recent research shows that changes on the long-range atomic order degree also affect the MT and Curie temperatures, due to the modification of both the electronic structure and the lattice sites occupancy by the magnetic atoms [5-11]. The simplest way to modify atomic order is by subjecting an alloy to different thermal treatments. In this sense it has been shown that quenching from high temperatures (around the B2-$L2_1$ ordering temperature) allows to partially retain the low atomic order present at these temperatures, in such a way that the $L2_1$ order degree on the as-quenched alloys is lower than the equilibrium value obtained after a slow enough cooling treatment. Likewise, if the as-quenched alloys are heated up to temperatures at which atomic diffusion is possible, an ordering process takes place leading to the restoring of the equilibrium atomic order degree of the alloy. In Ni-Mn-Ga the atomic diffusion needed for the ordering is mediated by vacancies [12]. During the quenching process an unknown amount of vacancies are retained. These vacancies control any ordering process, and indirectly the main properties of the MT, but the way vacancies assist the ordering process is still unclear. Besides, the vacancy parameters change during the different standard thermo-mechanical processes used in these materials. Positron annihilation spectroscopy (PALS) is a very powerful technique to investigate vacancy-type defects in metals. Depending on the material, PALS allows the measurement of the vacancy concentration between 0.1 and 1000ppm [13]. Therefore, this technique could allow to discriminate between ordering and vacancy dynamics and consequently to better understand vacancy assisted processes taking place in these materials. The main objective of this work is to show the role the vacancies play in Ni-Mn-Ga FSMA through the evaluation of the vacancy concentration, their kinetics (activation energies) and their temperature dependence when the sample are subjected to different treatments.

A polycrystalline ingot of Ni-Mn-Ga was prepared from high purity elements by arc melting under protective argon atmosphere. The ingot was homogenized in vacuum quartz ampoules at 1173 K during 24 hours. The measured alloy composition was $Ni_{53}Mn_{26}Ga_{21}$. Several samples extracted from the ingot were quenched from different temperature between

673-1173 K into ice water in order to produce a large quantity of quench-in defects. The time evolution of the vacancy concentration at 523 K, 573 K and 623 K was subsequently analysed in the samples quenched from 1173 K. Positron lifetime measurements were performed by PALS always at room temperature after the different thermal treatments. A fast-fast system with a resolution of 250ps and a conventional ^{22}Na source on a kapton foil, employed as the positron source, were used for positron lifetime measurements. The positron source was sandwiched between two identical samples. All lifetime spectra were analyzed after subtracting the constant source contribution (382ps 17% and 1600ps 1%). The statistic of each spectrum was always better than 1.6 million counts.

Positrons emitted from the source penetrate the sample and annihilate at a constant rate if the material is defect free. In this case the measured positron annihilation distribution corresponds to a single exponential, where the exponential factor is the annihilation rate. The inverse of this annihilation rate is the positron lifetime in the bulk, τ_B .When positron traps (vacancies) are present in the material a combination of two exponentials are measured. The lifetime of the first exponential, τ_1, is related to positron annihilation from the bulk and to the trapping rate of positrons by vacancies, κ_v [14]. The second lifetime, τ_2, is the positron lifetime in the vacancy, τ_v. The lifetime in the vacancy is always longer that the lifetime in the bulk. The lifetime spectra is analyzed using two lifetime components, $n(t)=I_1/\tau_1 \times e^{-t/\tau 1} + I_2/\tau_2 \times e^{-t/\tau 2}$. These two exponentials have different intensities: I_1 and I_2, being $I_1+I_2=1$. The measured τ_1, τ_2, I_1 and I_2 allow determining the values of τ_B, τ_v and κ_v according to the following equations [14]:

$$\tau_1 = \frac{\tau_B}{1+k_v \times \tau_B} \quad (1)$$

$$\tau_2 = \tau_v \quad (2)$$

$$I_2 = \frac{k_v}{\frac{1}{\tau_B} - \frac{1}{\tau_v} + k_v} \quad (3)$$

These relations summarize the well known one trap model [13]. The statistically important average lifetime $\tau_{Av} = \tau_1 \cdot I_1 + \tau_2 \cdot I_2$ (which can be estimated with an error of 1ps) allows to know the vacancy concentration according to the following expression:

$$k_v = \frac{1}{\tau_B} \times \frac{\tau_{AV} - \tau_B}{\tau_v - \tau_{AV}} = \mu_v \times C_v \quad (4)$$

Where μ_v is the specific trapping rate and depends slightly on the material. A value $1.5 \times 10^{14} s^{-1}$ is used for Niquel [15,16].

The vacancy concentration depends on the thermal history of the sample. In a first approximation, the vacancy concentration in thermal equilibrium, as a function of temperature, can be expressed as a Boltzmann´s relation $C_v = A \times \exp\left(\frac{-E_F}{k_{\mathbf{B}}T}\right)$ where A is usually refereed as the pre-exponent factor, E_F is the formation energy, $k_{\mathbf{B}}$ is the Boltzmann constant and T is the temperature. On the other side, when the vacancy concentration is out of the equilibrium a time dependence can be considered according to $C_v = C_0 \times \exp\left(\frac{-t}{\theta}\right) + C_{eq}$ [16], where C_0 is the concentration of vacancies at t=0, C_{eq} is the thermal equilibrium vacancy concentration at such a temperature and θ is a characteristic relaxation time that can be expressed in terms of the migration energy by $\theta = \theta_0 \times \exp\left(\frac{E_M}{k_{\mathbf{B}}T}\right)$ where θ_0 is a constant [17].

Figure 1 shows the average positron lifetime, measured as a function of the annealing time, at three different temperatures 523 K, 573 K and 623 K, after quenching from 1173ºC. For the three temperatures the average positron lifetime can be fitted to a straight line. The higher the temperature is, the higher the slope of the lines.

To establish a quantitative relation between the average positron lifetime and the vacancy concentration it is necessary to determine the positron lifetime at the vacancy and at the bulk, see equation (4). Figure 2 shows the time evolution of the components of the average lifetime at 523 K after quenching from 1173 K. For short annealing times one single component is present ($\tau_2 = \tau_v$=181±2ps). This value indicates that positrons are trapped at vacancy type defects [18]. For longer annealing times two exponentials are present. The longer lifetime is the one related to vacancy type defects (τ_2). Its lifetime remains constant up to the highest annealing time used in the measurements. However, the shorter lifetime τ_1, which is related to τ_B, and the trapping rate κ_v, increases with annealing time. Figure 2 also shows the intensity of the first and second lifetimes (I_1 and I_2). I_2 decreases from 100% at the beginning to 78% at 16ks. This indicates that the vacancy concentration decreases as the annealing time increases. Using the values of figure 2, a bulk positron lifetime of τ_B =136±2ps has been estimated. In the studied sample three different type of vacancies (monovacancies) could be present: V_{Ni}, V_{Mn} and V_{Ga}, However, taking into account that, first, the long lifetime component remains constant for all the performed thermal treatments and second, the one trap model fits the positron spectra decomposition results (the obtained bulk lifetime remains constant), only one vacancy type defect has to be considered. This experimental result can be due to the existence of only one predominant vacancy type defect or, in the case that more vacancy type defects were the predominant ones, their positron lifetimes are very similar and

close to the long lifetime (181±2ps). This value is associated to monovacancies [18] and it is the unique effective vacancy type defect for positrons in the present study.

Figure 3 shows the relation between the vacancy concentration and the average lifetime obtained using equation 4. This figure establishes the upper and lower limits of the concentration of vacancies that can be measured in the samples by PALS. For instance, for samples whose measured average lifetime is 3ps lower than the maximum lifetime (vacancy lifetime, 181ps) or 3ps higher than the minimum lifetime (bulk lifetime, 136ps) , the range in the vacancy concentration that this technique could measure is between 670ppm and 3ppm, respectively. Figure 3 combined with the results presented in Figure 1 allows to obtain the vacancy concentration as a function of the annealing time at different temperatures. Figure 4 shows the vacancy concentration as a function of the annealing time for the three annealing temperatures. There exists a linear correlation between the logarithm of the vacancy concentration and the annealing time for each temperature. The slope of every linear fitting is the inverse of the characteristic relaxation time θ of the elimination of vacancies for each particular temperature, as previously remarked. The values obtained are: 3500±200 s, 1100±60 s and 490±20 s for 250 ºC, 300 ºC and 350ºC annealing temperatures, respectively.

The characteristic relaxation times, θ, can be used to obtain the activation energy of the vacancy migration [17]. The inset in figure 4 shows the Arrhenius plot of the relaxation time, θ. The vacancy migration energy obtained from the plot, which is directly associated with the vacancy elimination during the annealing process, is 0.55±0.05eV. As far as the authors know there are not previous experimental references in the literature about the vacancy migration energy in Ni-Mn-Ga samples. Regrettably, the results of PALS in the present work do not allow differentiating between the three possible types of vacancies: V_{Ni}, V_{Mn} and V_{Ga} , but the fact that the vacancy concentration changes with temperature as a single exponential decay confirms the previous assumption that there is only one effective vacancy type defect for positrons. Now, since the three isothermal annealing treatments were performed after quenching from the same temperature (1173 K), the vacancy concentration at the initial time (t=0) must be the same. In fact, the linear fittings in figure 4 coincide at the same point in the ordinate axis. This point gives an initial vacancy concentration of 1100±200ppm at room temperature for the sample quenched from 1173 K.

Finally, figure 5 shows the average positron lifetime at room temperature (right axis) and the vacancy concentration (left axis) as a function of the quenching temperature. The average lifetime increases with temperature in the 673 K - 873 quenching temperature range. Above 873 K the measured average lifetime keeps constant up to 1173 K since the vacancy

concentration above 873 K is higher than the upper limit of the sensibility of the technique, see figure 3. Using equation 4, the vacancy concentration in the as-quenched state can be estimated. Figure 5 shows that the vacancy concentration increases from 11ppm to 200ppm, when quenching temperature increases from 673 K to 823 K.

In order to evaluate the vacancy lost in the quenching process, the characteristic relaxation time θ can be estimated for different temperatures using the previous equation $\theta = \theta_0 \times \exp\left(\frac{E_M}{k_B T}\right)$, from which the time dependence of the vacancy concentration can be evaluated. For instance, the relaxation time θ at 873 K can be estimated to be 26s, so even if the sample needs 1s for cooling from 873 K to room temperature through the quenching process, at least 97% of the vacancies presented should be retained. On quenching from temperatures lower than 873 K the percentage of the retained amount of vacancies must be higher. Due to the large quenching rate used, the measured vacancy concentration in the as-quenched state may not differ too much from that of the equilibrium at the different quenching temperatures and the Boltzmann´s relation described above can be used to determine the vacancy formation energy. The inset in figure 5 shows the Arrhenius plot of the concentration of vacancies for the data in figure 5. From this plot vacancy formation energy of 0.90±0.07eV is obtained. Therefore, the self-diffusion activation energy (formation plus migration energies) measured in this work for the effective vacancy is 1.45±0.07eV. This value is very close to the one obtained for the self-diffusion activation energy for Ni and Mn by Erdélyi et al. [12] (1.49±0.05eV and 1.46±0.05eV, respectively), using tracers lattice diffusion measurements, and quite different to the one obtained for Ga atoms [12]. This could indicate that the mayor contribution to the effective vacancy defect we are measuring in the present work comes from the Ni and/or Mn vacancies.

In summary, positron annihilation spectroscopy (PALS) has demonstrated to be a powerful technique to study vacancies in ferromagnetic shape memory alloys. The analysis on a Ni-Mn-Ga alloy subjected to several thermal treatments has allowed us to determine the vacancy concentration and their kinetics. The concentration of retained vacancies increases as the quenching temperature becomes higher. 1100±200ppm of vacancies are retained in the as-quenched state of a sample quenched from 1173 K. The vacancy migration and formation energies are 0.55±0.05eV and 0.90±0.07eV respectively for a $Ni_{53}Mn_{26}Ga_{21}$ sample.

ACKNOWLEDGMENTS

This work has been carried out with the financial support of the Spanish "Ministerio de Economía y Competitividad" and the Basque Government grants: MAT2012-37923 and IT-443-10

REFERENCES

[1]K. Ullakko, J. K. Huang,C. Kantner,R.C. O'Handley and V.V. Kokorin, Appl. Phys. Lett. **69**, 1966 (1996)

[2]K. M. Mostafa, N. Van Caenegem,J. de Baerdemaeker,D. Segers and Y Houbaert, Physica Status Solidi (c) **4** 3554 (2007)

[3]K. Oikawa,T. Ota,T. Ohmori,Y. Tanaka,H. Morito,A. Fujita,R. Kinuma,K. Fukamichi and K. Ishida, Appl. Phys. Lett **81**, 5201 (2002)

[4]V. A. Chernenko Scr. Mater **40** 523 (1999)

[5]R. W. Overholser, M. Wuttig and D. A. Neumann, Scr. Mater. **40** 1095 (1999)

[6]M. Kreissl,K. U. Neumann,T. Stephens and K. R. Ziebeck, J. Phys: Condens. Matter. **15** 3831 (2003)

[7]T. Goryczka,M. Gigla and H. Morawiec Int. J. Appl. Elect. Mech. **23** 81 (2006)

[8]V. Sánchez-Alarcos,J. I. Pérez-Landazábal, V. Recarte and G. J. Cuello Acta Mater. **55** 3883 (2007)

[9]V. Sánchez-Alarcos, J. I. Pérez-Landazábal, C. Gómez-Polo and V. Recarte J. Magn. Magn. Mater. **320** e160 (2008)

[10]V. Sánchez-Alarcos, J. I. Pérez-Landazábal, V. Recarte, J. A. Rodríguez-Velamazán and V. A. Chernenko J. Phys.: Condens. Matter. **22** 166001 (2010)

[11]V. Sánchez-Alarcos, J. I. Pérez-Landazábal and V. Recarte, Mater. Sci. Forum **684** 85-103 (2011)

[12]G.Erdélyi, H.Mehrer, A.W.Imre, T.A.Lograsso and and D.L.Schlagel, Intermetallics **15** 1078-1083(2007)

[13]A. Dupasquier, G. Kögel and A. Somoza Acta Mater **52** 4707 (2004)

[14]A.Vehanen, P. Hautojärvi and J. Yli-Kauppila, Phys. Rev. B. **25** 762 (1982)

[15]H. E. Schaefer Phys. Stat. Sol. (a) **102** 47 (1987)

[16]Staab, R. Krause-Rehberg, B. Vetter and B. Kieback , Journal of Physics: Condensed Matter, **11**, 7, 1807 (1999)

[17]A.C. Damask and G. J. Dienes, Point Defects in Metals, (1971)

[18]J. M.Campillo, J.M. Ogando and F.Plazaola, J. Phys.: Condens. Matter **19** 176222 (2007)

Figure Captions

Figure 1: Positron average lifetime τ_{Av} for three different temperatures as a function of annealing time 523 K (square), 573 K (circle) and 623 K (diamond) for the sample quenched from 1173 K. The straight lines show the linear fit for the experimental values.

Figure 2: Decomposition of the positron average lifetime for the annealing at 523 K in figure 1. τ_1(closed squares), τ_2(closed circles), I_1 (open squares) and I_2 (open circles).

Figure 3: Relation between vacancy concentration and measured average lifetime obtained by means of equation 4.

Figure 4: Vacancy concentration (logarithmic scale) for annealing temperatures of 523 K (diamond), 573 K (circle) and 623 K (square) versus annealing time. Inset: Linear fit of the relaxation times of figure 4 versus the inverse of the temperature.

Figure 5: Vacancy concentration in logarithmic scale (full squares in left axis) and the corresponding average lifetime (empty squares in right axis) as a function of quenching temperature. Inset: Linear fit of the logarithm of the vacancy concentration versus the inverse of the quenching temperature.

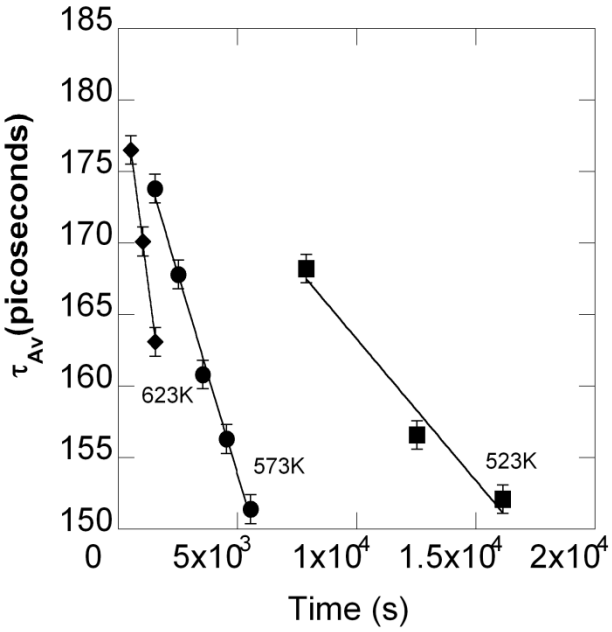
185
180
175
170
165
160
155
150
τ_{Av}(picoseconds)
623K
573K
523K
0
5x10^3
1x10^4
1.5x10^4
2x10^4
Time (s)

Figure 1

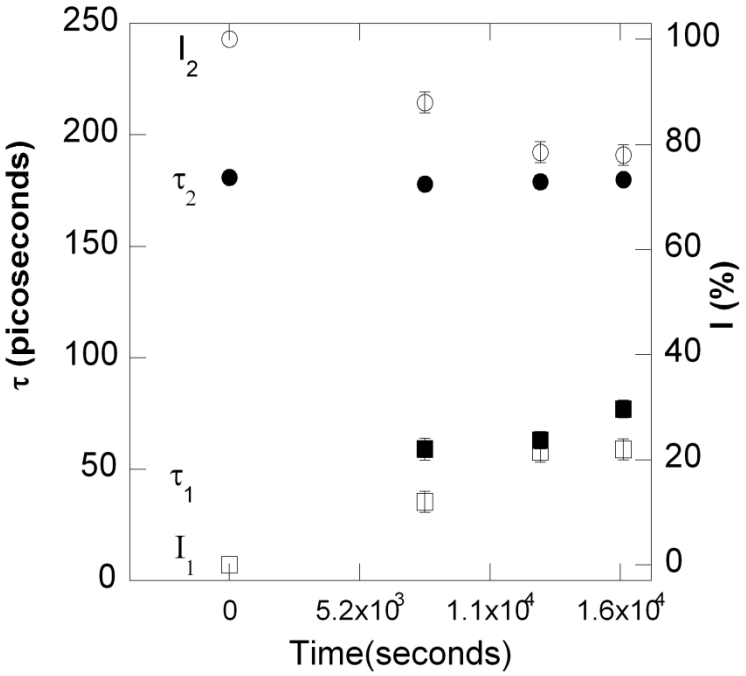
250
200
150
100
50
0
τ (picoseconds)
100
80
60
40
20
0
I (%)
I2
τ2
τ1
I1
0
5.2x10^3
1.1x10^4
1.6x10^4
Time(seconds)

Figure 2

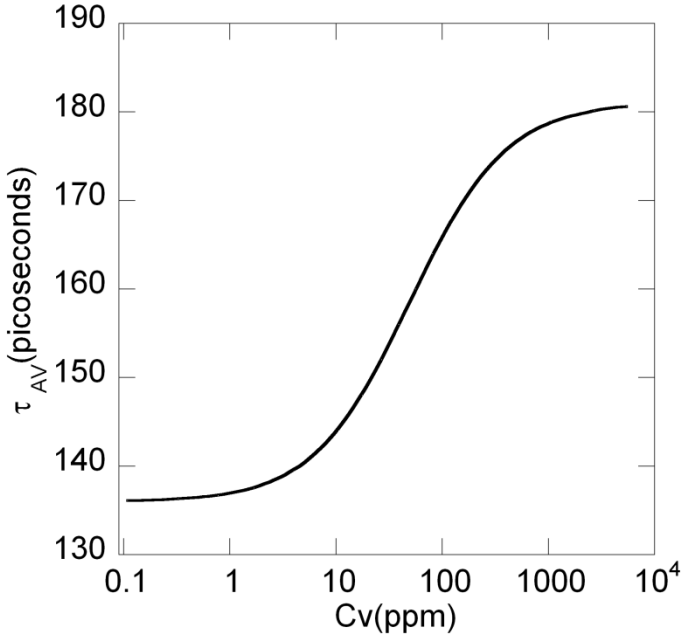
190
180
170
160
150
140
130
τ AV (picoseconds)
0.1
1
10
100
1000
10^4
Cv(ppm)

Figure 3

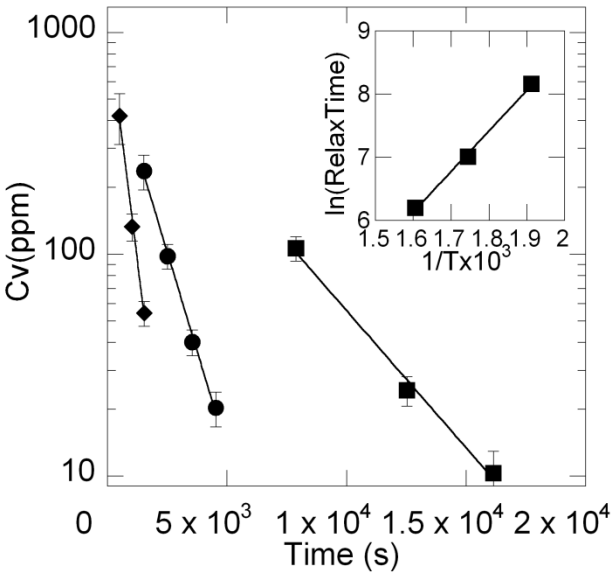
1000
100
10
Cv(ppm)
0
5 x 10^3
1 x 10^4
1.5 x 10^4
2 x 10^4
Time (s)
9
8
7
6
ln(RelaxTime)
1.5
1.6
1.7
1.8
1.9
2
1/Tx10^3

Figure 4

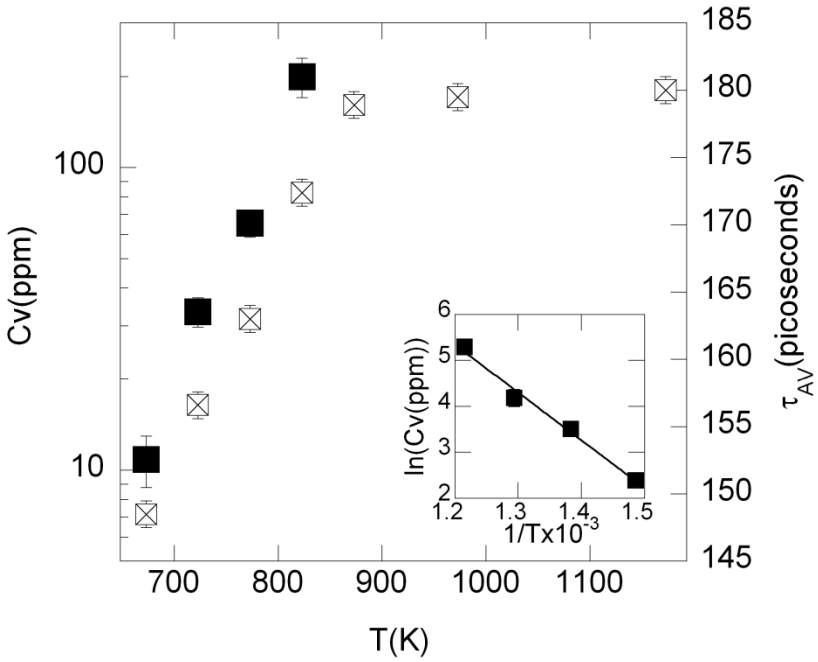
Cv(ppm)
100
10
700
800
900
1000
1100
T(K)
185
180
175
170
165
160
155
150
145
τAV(picoseconds)
ln(Cv(ppm))
6
5
4
3
2
1.2
1.3
1.4
1.5
1/Tx10-3

Figure 5